

Fast energy transfer within a self-assembled cyclic porphyrin tetramer†

Rebecca A. Jensen,^{ab} Richard F. Kelley,^{ab} Suk Joong Lee,^{ab} Michael R. Wasielewski,^{*ab} Joseph T. Hupp^{*ab} and David M. Tiede^{bc}

Received (in Berkeley, CA, USA) 3rd December 2007, Accepted 27th February 2008

First published as an Advance Article on the web 20th March 2008

DOI: 10.1039/b718628b

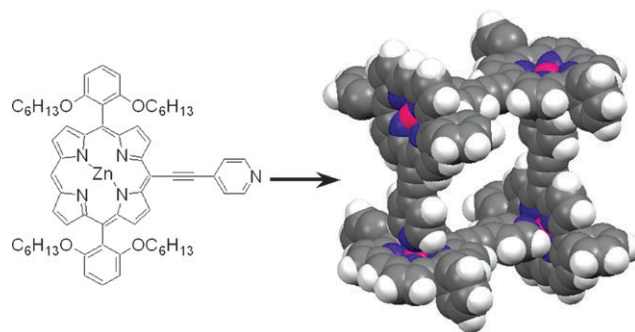
The structure of a cyclic self-assembled tetramer of an asymmetric *meso*-ethynylpyridyl-functionalized Zn(II)-porphyrin was established by solution-phase X-ray scattering and diffraction; femtosecond transient absorption and anisotropy spectroscopies were used to (a) observe rapid energy transfer (3.8 ps^{-1}) between porphyrin subunits and (b) establish that the transfer occurs between adjacent units.

Porphyrins have often been employed as light-harvesters—both in bio-inspired model systems¹ and in energy-converting photoelectrochemical systems.² Their appeal stems from their large extinction coefficients and relative ease of synthesis and modification, as well as their structural similarity to naturally occurring pigments such as chlorophylls and chlorins.³ Particularly interesting, for both fundamental and applied reasons, are *ensembles* of porphyrins.⁴ From an applications perspective, the attachment of multi-porphyrin structures to electrode surfaces, as opposed to single, non-aggregated chromophores, may be useful for controlling dye spacing and orientation and for modulating dye coverage and dye-layer porosity.⁵ Additionally, if energy transfer (EnT) between porphyrins is sufficiently rapid, ensembles can function as light-harvesting antennae in much the same fashion as in natural photosynthetic systems.⁶ Here we report on EnT within a photo-excited porphyrin ensemble comprising a self-assembling cyclic tetramer. The solution-phase structure of the tetramer is established *via in situ* X-ray scattering and diffraction measurements. We demonstrate that very small structural changes, relative to previously investigated tetramers,⁷ lead to substantially faster EnT. Additionally, we show that by combining data from polarized transient absorption experiments with data from singlet–singlet annihilation experiments, the relative importance of EnT for adjacent *versus* parallel porphyrin subunits can be determined.

EnT within self-assembled porphyrin arrays generally occurs *via* Förster resonance energy transfer (through-space transfer), the efficiency of which is determined by the distance

and orientation between the donor and acceptor transition dipole moments and the overlap of donor absorption and acceptor emission spectra.⁸ Adjustments of these parameters are achieved through modification of porphyrin unit and assembly schemes for the optimization of energy capture and transfer. Here, *meso*-ethynylpyridyl-functionalized Zn(II)-porphyrin (**EPZn**), synthesized in 31% yield by Sonogashira coupling of 4-ethynylpyridine and *meso*-bromo Zn(II)-porphyrin (see ESI†), is used as an ensemble building block. The resulting supramolecular complex has been characterized by solution-phase UV-Vis and fluorescence spectroscopy, ¹H NMR spectrometry, small-angle X-ray scattering (SAXS), and wide-angle X-ray scattering (WAXS).

The tetrameric cyclic ensemble proposed for **EPZn** spontaneously assembles by coordination of substituent-ethynylpyridyl nitrogens and porphyrin Zn(II) sites (Scheme 1). The ground-state electronic absorption spectrum of **EPZn** in dry toluene was observed to red-shift with increasing concentration up to 110 μM with Soret, Q_x , and Q_y bands at 447, 575, and 629 nm, respectively (ESI† Fig. S2). The absorbance of Zn-porphyrin is known to red-shift upon coordination of the central porphyrin Zn(II) metal with electron-donating ligands, such as pyridine.⁹ In dry toluene, the **EPZn** ethynylpyridyl nitrogen is the only donor available for binding, and the observed red-shift in absorbance is attributed to the formation of a multi-porphyrin species. The Q_x and Q_y band positions at 110 μM are 15 and 25 nm to the red of those of a self-assembled Zn-porphyrin cyclic tetramer featuring direct attachment of pyridyl groups to *meso* porphyrin sites.⁷ In addition, considerable intensification of the lower-energy Q_y band is seen relative to the Q_x band. This is a consequence of the greater degree of symmetry reduction introduced by the 4-ethynylpyridyl substituent in **EPZn** which makes the normally



Scheme 1 Assembly of **EPZn** cyclic tetramer in a non-coordinating solvent. Solubilizing groups of the space-filling tetramer model (right) have been omitted for clarity.

^a Department of Chemistry, Northwestern University, 2145 Sheridan Road, Evanston, IL 60208, USA. E-mail: j-hupp@northwestern.edu. E-mail: m-wasielewski@northwestern.edu; Fax: +1-847-467-1425; Tel: +1-847-491-3504

^b Argonne-Northwestern Solar Energy Research (ANSER) Center, Northwestern University, 2145 Sheridan Road, Evanston, IL 60208, USA

^c Chemistry Division, Argonne National Laboratory, Argonne, IL 60439, USA

† Electronic supplementary information (ESI) available: Details of synthesis, characterization, and additional transient absorption and anisotropy data. See DOI: 10.1039/b718628b

forbidden Q bands, especially the Q_y band, more allowed.¹⁰ The red shift and increase in oscillator strength of the lowest energy transition enhance the overlap of the absorption and emission spectra (Fig. 1).

Additional evidence for self-assembly is provided by comparisons of **EPZn** ^1H NMR spectra in non-coordinating and coordinating solvents (ESI† Fig. S3). In toluene- d_8 , coordination between the ethynylpyridyl nitrogen and Zn(II) places the α and β pyridyl-protons within the ring current of the coordinated porphyrin, resulting in shielded proton resonances (5.42 and 2.69 ppm).¹¹ Upon addition of 10 molar equivalents of pyridine- d_5 , the structure disassembles, and the pyridyl-proton resonances shift downfield (9.83 and 7.36 ppm).

Definitive evidence for the proposed tetrameric ensemble was obtained from solution-phase SAXS measurements carried out over a q range of 0.01 to 0.43 \AA^{-1} . In the low q region ($q < 0.2 \text{ \AA}^{-1}$), the scattering intensity follows the Guinier relation that is parameterized in terms of the forward scattering amplitude, $I(0)$, and the radius of gyration, R_g :¹²

$$I(q) = I(0)\exp(-q^2 R_g^2/3) \quad (1)$$

Experimental R_g values were determined from least squares fits to the Guinier scatter plots. In dry toluene, the R_g value for **EPZn** is $10.5 \pm 0.2 \text{ \AA}$ (Fig. 2). This value decreased with the addition of 2 molar equivalents of pyridine to $4.6 \pm 0.1 \text{ \AA}$ (ESI† Fig. S4). These results matched R_g values calculated from the simulated scattering of geometry-optimized models¹³ for the tetramer (10.3 \AA) and pyridine-ligated monomer (4.6 \AA). Strain minimization clearly should favor a tetramer over other cyclic structures. Nevertheless, scattering was also modeled for hypothetical trimer and pentamer assemblies; these gave R_g values of 8.3 \AA and 11.6 \AA , respectively.

In addition to scattering, by extending the X-ray studies to wide-angle (large q : 0.11 to 2.37 \AA^{-1}), WAXS diffraction data were obtained. These data are most conveniently interpreted *via* atomic pair distribution (PDF) analyses, in either real or reciprocal space. PDF plots are often dominated by heavy atoms (in this case, zinc atoms). Experimental and tetramer-model PDFs, ob-

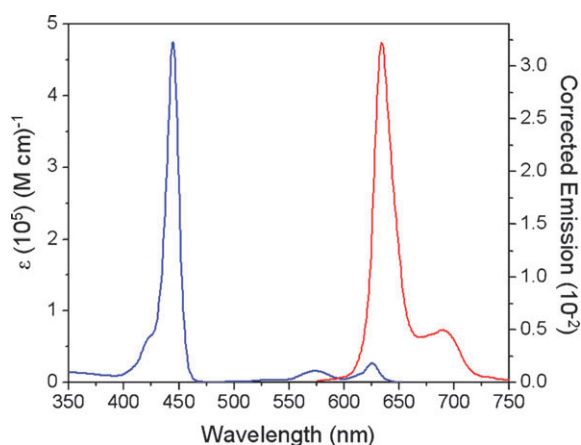


Fig. 1 Ground-state electronic absorption spectrum of **EPZn** in pyridine (blue) with peak positions: 444 nm (Soret), 573 nm (Q_x), 625 nm (Q_y), and excited-state electronic emission spectrum of **EPZn** in pyridine (red) with 553 nm excitation and total intensity normalized to unity, with peak positions: 634 nm (Q_y) and 688 nm.

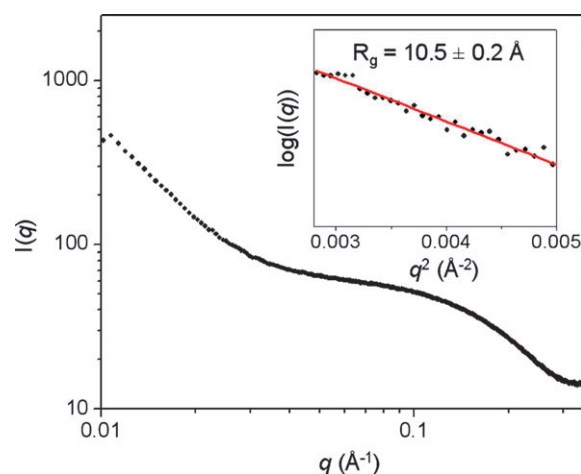


Fig. 2 Experiment scattering intensity, $I(q)$, versus scattering vector, q , data for **EPZn** in dry toluene. Inset: Scattering intensity versus q^2 . Guinier fit to the data is also shown.

tained using the X-ray scattering fitting program GNOM,¹⁴ matched with peaks at 13.6 and 19.4 \AA that correspond to the distance between adjacent and diagonal porphyrin units, respectively (Fig. 3). These values are $\sim 6\%$ larger than the Zn–Zn distances of the tetramer model (12.9 and 18.2 \AA) due to electron density contributions from the porphyrin rings and substituents. The sinusoidal behavior observed in the experimental PDF plot around 23 \AA is due to truncation artifacts of the Fourier transform. Model Zn–Zn distances are displayed in the PDF derived from only the Zn-metal atoms in the model (ESI† Fig. S5).

Transient absorption data were collected for **EPZn** in dry toluene and in pyridine following excitation with 632 nm, 120 fs laser pulses. The decay kinetics of $^1\text{EPZn}$ in dry toluene were biexponential, with $\tau = 3.2 \pm 0.2 \text{ ps}$ and $\tau = 2.5 \text{ ns}$ (Fig. 4). In pyridine, the decay kinetics of $^1\text{EPZn}$ were monoexponential with $\tau = 2.5 \text{ ns}$ (ESI† Fig. S6). The 2.5 ns decay component in both dry toluene and pyridine matches the measured fluorescent lifetime in pyridine (ESI† Fig. S8).

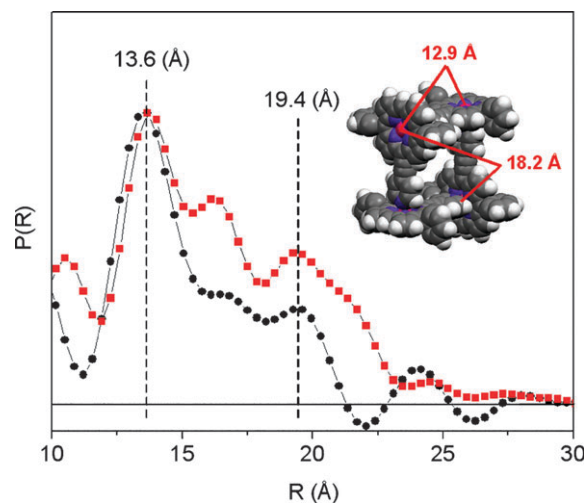


Fig. 3 Experiment (black) and tetramer model (red) pair-distribution plots, calculated from corresponding X-ray scattering intensity versus q (\AA^{-1}) plots. Inset: **EPZn** tetramer model (solubilizing groups omitted) with adjacent and diagonal Zn–Zn distances indicated.

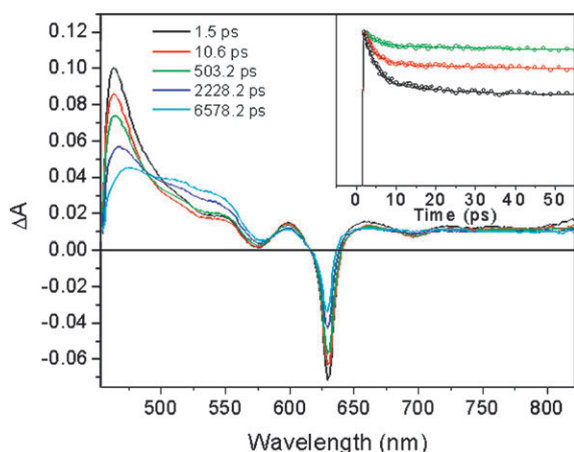


Fig. 4 Transient absorption spectra of **EPZn** in dry toluene following excitation with 632 nm, 120 fs laser pulses. Inset: power dependent transient absorption kinetics of $^1\text{EPZn}$ monitored at 466 nm using 1.00 (black), 0.66 (red), and 0.33 (green) μJ per 632 nm excitation pulse.

The amplitude of the 3.2 ps decay component in dry toluene was found to be laser power dependent, indicative of single–singlet annihilation (inset Fig. 4). The following formula relates the annihilation lifetime (τ_a) to the EnT lifetime (τ_h) for cyclic arrays made up of N chromophores:¹⁵

$$\tau_a = \tau_h / (8 \sin^2(\pi/2N)) \quad (2)$$

Using this model, $N = 4$, and the measured τ_a , an EnT lifetime of 3.8 ± 0.2 ps was determined.

In the limit where the transition dipole moment becomes completely polarized along the ethynylpyridyl axis, the moments of adjacent porphyrins would be essentially orthogonal, with the dynamics of EnT greatly decreased. Under those conditions, EnT conceivably could be dominated instead by dipolar coupling between parallel porphyrins, *i.e.* porphyrins comprising opposite sides of a tetrameric assembly. Disfavoring the coupling, however, would be the comparatively large separation distance between the candidate energy donor and acceptor. To differentiate between the two possible pathways of EnT, transient absorption anisotropy measurements were conducted. The depolarized nature of the experiment allows only EnT between the perpendicularly oriented adjacent **EPZn** tetramer units to be observed. The transient absorption depolarization lifetime ($\tau_{\text{depolarization}}$) is related to the EnT lifetime by the following equation:¹⁶

$$\tau_h = 4(1 - \cos^2 \alpha) \tau_{\text{depolarization}} \quad (3)$$

where α is the angle between the donor and acceptor species. The value of $\tau_{\text{depolarization}}$ obtained for **EPZn** in dry toluene was 1.1 ± 0.1 ps, revealing an EnT lifetime of 4.4 ± 0.4 ps (ESI† Fig. S7). This matches (within experimental error) the EnT lifetime result obtained from the annihilation experiment, demonstrating that EnT occurs chiefly between adjacent units of the **EPZn** cyclic tetramer.

The rate of EnT within the **EPZn** cyclic self-assembled tetramer is ~ 8 times faster than that reported for a closely analogous Zn(II)–porphyrin tetramer with direct *meso*-pyridyl functionalization.⁷ Introduction of an ethynyl group between the porphyrin and pyridyl rings increases the distance between

porphyrin units by ~ 2.6 Å, but also enhances the strength of the transition dipole moment along the direction of the ethynylpyridyl substituent. The porphyrin symmetry is reduced which enhances the overlap of absorption and emission spectra. A similar EnT enhancement was observed within a cyclic chlorophyll tetramer,¹⁷ where the rate of energy transfer (1.2 ± 0.1 ps) was observed to be ~ 20 times faster than that of the *meso*-pyridyl Zn(II)–porphyrin tetramer. This difference was attributed to the larger transition dipole moment found in chlorophyll as compared to porphyrin. Further increasing the conjugation within the porphyrin tetramer units and/or varying the transition dipole moment orientations within the assembly may result in even faster EnT rates. We are currently designing new porphyrin systems to investigate this possibility.

We thank the Office of Science, US Department of Energy for support of our work (Grants DE-FG02-87ER13808 and DE-FG02-99ER14999 to Northwestern and contract W-31-109-ENG-38 to the Argonne National Laboratory). We are especially appreciative of the expert help of the Sector 12 staff at the Advanced Photon Source.

Notes and references

- (a) H. Imahori, Y. Sekiguchi, Y. Kashiwagi, T. Sato, Y. Araki, O. Ito, H. Yamada and S. Fukuzumi, *Chem.–Eur. J.*, 2004, **10**, 3184; (b) A. Harriman, *Angew. Chem., Int. Ed.*, 2004, **43**, 4985; (c) M. J. Ahrens, R. F. Kelley, Z. E. X. Dance and M. R. Wasielewski, *Phys. Chem. Chem. Phys.*, 2007, **9**, 1469–1478; (d) R. F. Kelley, W.-S. Shin, B. Rytchinski and M. R. Wasielewski, *J. Am. Chem. Soc.*, 2007, **129**, 3173–3181.
- (a) Y. Tachibana, S. A. Haque, I. P. Mercer, J. R. Durrant and D. R. Klug, *J. Phys. Chem. B*, 2000, **104**, 1198–1205; (b) F. Odobel, E. Blart, M. Lagree, M. Villieras, H. Roujtita, N. E. Murr, S. Caramori and C. A. Bignozzi, *J. Mater. Chem.*, 2003, **13**, 502–510; (c) W. M. Campbell, A. K. Burrell, D. L. Officer and K. W. Jolley, *Coord. Chem. Rev.*, 2004, **248**, 1363–1379.
- L. R. Milgrom, *The Colours of Life*, Oxford University Press, Oxford, UK, 1997.
- K. Ogawa and Y. Kobuke, *J. Photochem. Photobiol. C: Photochem. Rev.*, 2006, **7**, 1–16.
- (a) A. B. F. Martinson, A. M. Massari, S. J. Lee, R. W. Gurney, K. E. Splan, J. T. Hupp and S. T. Nguyen, *J. Electrochem. Soc.*, 2006, **153**(3), A527–A532; (b) A. M. Massari, R. W. Gurney, C. P. Schwartz, S. T. Nguyen and J. T. Hupp, *Langmuir*, 2004, **20**, 4422–4429; (c) K. E. Splan, A. M. Massari and J. T. Hupp, *J. Phys. Chem. B*, 2004, **108**, 4111–4115; (d) J. Libera, R. Gurney, C. Schwartz, H. Jin, T.-L. Lee, S. T. Nguyen, J. T. Hupp and M. Bedzyk, *J. Phys. Chem. B*, 2005, **109**, 1441–1450.
- G. McDermott, S. M. Prince, A. A. Freer, A. M. Hawthornthwaite-Lawless, M. Z. Papiz, R. J. Cogdell and N. W. Isaacs, *Nature*, 1995, **374**, 517.
- (a) M. M. Yatskou, R. B. M. Koehorst, H. Donker and T. J. Schaafsma, *J. Phys. Chem. A*, 2001, **105**, 11425–11431; (b) M. M. Yatskou, R. B. M. Koehorst, A. van Hoek, H. Donker, T. J. Schaafsma, B. Gobets, I. van Stokkum and R. van Grondelle, *J. Phys. Chem. A*, 2001, **105**, 11432–11440.
- J. R. Lakowicz, *Principles of Fluorescence Spectroscopy*, Kluwer, Dordrecht, 1999.
- (a) P. N. Taylor and H. L. Anderson, *J. Am. Chem. Soc.*, 1999, **121**, 11538–11545; (b) H. L. Anderson, *Inorg. Chem.*, 1994, **33**, 972–81.
- M. Gouterman, *J. Phys. Chem.*, 1959, **30**, 1139–1161.
- G. S. Wilson and H. L. Anderson, *Chem. Commun.*, 1999, 1539–1540.
- A. Guinier and G. Fournet, *Small-Angle Scattering of X-rays*, Wiley, New York, 1955.
- Hyperchem, version 5.02*, Hypercube Inc., Gainesville, FL, 1997.
- D. I. Svergun, *J. Appl. Crystallogr.*, 1992, **25**, 495–503.
- G. Trinkunas, *J. Lumin.*, 2003, **102–103**, 532–535.
- S. E. Bradforth, R. Jimenez, F. van Mourik, R. van Grondelle and G. R. Fleming, *J. Phys. Chem.*, 1995, **99**, 16179–16191.
- R. F. Kelley, R. H. Goldsmith and M. R. Wasielewski, *J. Am. Chem. Soc.*, 2007, **129**, 6384–6385.